

## Striped phases in two-dimensional dipolar ferromagnets

A. B. MacIsaac and J. P. Whitehead

*Department of Physics, Memorial University, St. John's, Newfoundland, Canada A1B 3X7*

M. C. Robinson and K. De'Bell

*Department of Physics, Trent University, Peterborough, Ontario, Canada K9J 7B8*

(Received 22 July 1994; revised manuscript received 10 November 1994)

A uniaxial spin system on the square lattice, where the spins are oriented perpendicular to the lattice and are coupled by both a dipole-dipole interaction and an exchange interaction, is studied. The subtle interplay of the exchange and dipolar interaction in two dimensions destabilizes the ferromagnetic ground state of the nearest-neighbor Ising model and gives rise to a sequence of striped phases. An analytic expression for the leading terms in an asymptotic expansion of the ground-state energy for the striped phase is derived for the discrete lattice. Comparison with the corresponding results for a previously proposed checkerboard state show that the striped phase is the ground state. The results are shown to be in excellent agreement with earlier numerical results. The finite-temperature phase diagram is obtained for a finite lattice using Monte Carlo simulation techniques and the corresponding structure-factor patterns discussed.

### I. INTRODUCTION

The interplay between a long-range dipolar interaction and a short-range exchange interaction can give rise to a variety of interesting and unusual magnetic phenomena. Recently Taylor and Gyffory<sup>1</sup> and, independently, the present authors<sup>2</sup> have noted that in the case of two dimensional magnetic systems in which the magnetic moments associated with the spins are aligned out of plane, this interplay could result in the appearance of striped phases. Taylor and Gyffory considered these systems as part of a study of magnetic ordering in metal-on-metal overlayers. The motivation for the present authors was the large number of experimental studies of magnetic ordering in the rare-earth subsystems of the high- $T_c$  superconductors and related layered compounds.<sup>3</sup> These studies were based on ground-state calculations for finite-size Ising systems. Previous work based on phenomenological theories<sup>4</sup> and continuum models of ultrathin films<sup>5,6</sup> had concluded that such phases would be stable with respect to the ferromagnetic state for all values of the exchange parameter. However, Taylor and Gyffory note the possibility that a finite value of the exchange parameter exists for the Ising system at which the ferromagnetic phase becomes stable. A previous study of an Ising system<sup>7</sup> concluded that the ground state in the presence of a dipolar interaction and large ferromagnetic exchange interaction is a checkerboard phase. We show that a full treatment of the discrete nature of the lattice clearly demonstrates that it is the striped phase which has the lowest energy.

In these striped phases the spins along a particular axis form a ferromagnetic chain, with spins on adjacent chains aligned to form ferromagnetic stripes of width  $ah$ , where  $a$  denotes the lattice constant. The magnetic moments in adjacent stripes are aligned in opposite directions to form an antiferromagnetic superlattice with modulation length  $\Lambda = 2ah$ . A striped phase corresponding to  $h = 4$  is shown schematically in Fig. 1.

In this paper we examine in more detail the phase behavior of such systems as a function of both the exchange coupling strength and temperature. In particular we obtain an analytic expression for the ground-state energy of the striped phases in the limit of large  $h$ . From this result we are able to show that the dipolar interaction will always destabilize the ferromagnetic ground state, against the formation of an antiferromagnetic striped phase, contrary to the phase diagram shown in Fig. 2 of Ref. 1. We also show that the width of the stripes increases exponentially with the strength of the exchange coupling. In addition to the results obtained for  $T = 0$ , we present the results of simulation studies carried out on a  $16 \times 16$  lattice from which we obtain some insight into the character of the finite-temperature phase diagram.

The outline of the paper is as follows. In Sec. II we present the Hamiltonian describing the energetics of the system of interest. In Sec. III we present numerical results for the energy per spin of the striped phase for finite  $h$  in the range  $1 \leq h \leq 400$ , and discuss its stability with

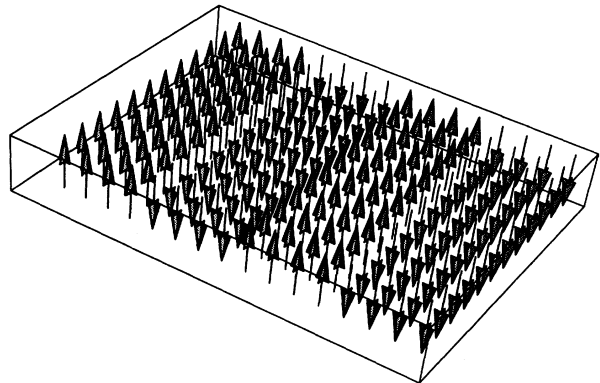


FIG. 1. The AF4 phase ( $h = 4$ ).

respect to the ferromagnetic phase. In Sec. IV we present an analytic expression for the ground-state energy in the limit of large  $h$ . It is shown that the resultant phase behavior agrees well with that obtained in the previous section, suggesting that corrections to the limiting form of the ground-state energy are small even for the lowest values of  $h$ . An explicit expression for the dependence of the equilibrium width of the stripes on the magnitude of the exchange coupling is given. The results of a similar analysis for the checkerboard phase is presented and it is shown that the striped phase has the lower energy for all values of coupling constant  $J$ . In Sec. V we present the finite-temperature phase diagram obtained from numerical simulations on a  $16 \times 16$  lattice. In the next section we present and discuss the diffraction patterns obtained from these simulations. Finally, in Sec. VII, we discuss what conclusions can be drawn from this work.

## II. HAMILTONIAN

We consider a two-dimensional system of uniaxial magnetic ions on a square lattice. The state of the magnetic ion, associated with the  $i$ th lattice site, is specified by the variable  $\sigma_i = \pm 1$ . Both the spin and the magnetic moment of the ions are assumed to be aligned perpendicular to the plane and are given by  $S_i = \sigma_i S_{\text{eff}}$  and  $\mu_i = \sigma_i \mu_{\text{eff}}$ , respectively, where  $S_{\text{eff}}$  and  $\mu_{\text{eff}}$  denote the effective spin and magnetic moments, respectively.

The magnetic ions are assumed to interact via a long-range dipole-dipole interaction and a short-range exchange interaction. The Hamiltonian may therefore be written as

$$\mathcal{H} = \mathcal{H}_{\text{ex}} + \mathcal{H}_{\text{dip}}, \quad (1)$$

where  $\mathcal{H}_{\text{ex}}$  contains terms involving the exchange interaction, and may be written as

$$\mathcal{H}_{\text{ex}} = -\mathcal{J} \sum_{\langle ij \rangle} S_i S_j, \quad (2)$$

where the summation over  $\langle ij \rangle$  denotes a sum over all nearest-neighbor pairs. The dipolar interaction  $\mathcal{H}_{\text{dip}}$ , may be written as

$$\mathcal{H}_{\text{dip}} = \frac{1}{2} \sum_{i \neq j} \frac{\mu_i \mu_j}{r_{ij}^3}, \quad (3)$$

where  $r_{ij}$  denotes the distance between the lattice sites  $i$  and  $j$  and the sum is a double sum where terms with  $i = j$  are excluded. Thus we have

$$\mathcal{H} = \frac{\mu_{\text{eff}}^2}{2a^3} E(\{\sigma_i\}), \quad (4)$$

where  $E(\{\sigma_i\})$  denotes the energy in dimensionless form, defined as

$$E(\{\sigma_i\}) = \sum_{i \neq j} \frac{\sigma_i \sigma_j}{R_{ij}^3} - J \sum_{\langle ij \rangle} \sigma_i \sigma_j, \quad (5)$$

where

$$R_{ij} = r_{ij}/a, \quad (6)$$

$$J = 2\mathcal{J}a^3 \left( \frac{S_{\text{eff}}}{\mu_{\text{eff}}} \right)^2. \quad (7)$$

For later use, we define the dipolar and exchange contributions as

$$E_{\text{dip}}(\{\sigma_i\}) = \sum_{i \neq j} \frac{\sigma_i \sigma_j}{R_{ij}^3}, \quad (8)$$

$$E_{\text{ex}}(\{\sigma_i\}) = -J \sum_{\langle ij \rangle} \sigma_i \sigma_j, \quad (9)$$

respectively.

## III. GROUND STATE

In the absence of the exchange interaction the ground state is simply an antiferromagnetic state with nearest-neighbor spins aligned in opposite directions. Introducing an antiferromagnetic exchange interaction ( $J < 0$ ) does not therefore change the ground-state spin configuration but simply serves to enhance the transition temperature. More interesting is the situation  $J > 0$ , since here one has competition between a long-range dipolar interaction favoring antiferromagnetic ordering and a short-range ferromagnetic interaction. In such a situation one might reasonably suppose that the ferromagnetic ground state would be stabilized for a sufficiently large value of  $J$ , leading to a phase diagram bounded by the antiferromagnetic phase at negative  $J$  and the ferromagnetic phase at large positive  $J$ , qualitatively similar to that obtained for the case in which the spins are aligned in the plane.<sup>8</sup> However, as shown by Refs. 1 and 2 this is not necessarily the case. Instead, for  $J > 0.85$  (in units of  $\mu_{\text{eff}}^2/2a^3$ ) we see the appearance of striped phases, similar to that shown schematically in Fig. 1 with the width of the stripes increasing with increasing  $J$ .

The exchange energy of the striped phase spin configuration may be readily calculated from the Hamiltonian given by Eq. (9) as

$$E_{\text{ex}}(h) = -2J \left( 1 - \frac{1}{h} \right). \quad (10)$$

The contribution from the dipole-dipole interaction  $E_{\text{dip}}(h)$ , given by Eq. (8), is somewhat more difficult to evaluate due to the long-range character of the interaction. However, by virtue of the periodic nature of the striped phase spin configuration, it is nevertheless possible to map the dipolar energy for the entire lattice to a sum within a single stripe. The resultant expression is given in Appendix A.

In Fig. 2 we graph the difference in the ground-state energy between the ferromagnetic state and the striped phase as a function of the exchange coupling  $J$ , for several values of  $h$ , together with the difference in energy between the ferromagnetic state and the antiferromagnetic state. From this we see that the ground state for  $J < 0.85$  is the antiferromagnetic state. At  $J = 0.85$ , the ground state changes from the antiferromagnetic to the striped phase, with  $h = 1$ . As the coupling constant  $J$  is increased further, we see that the ground state changes

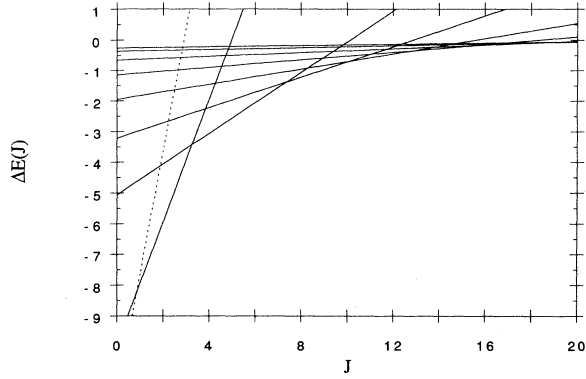


FIG. 2. The energy of the striped phases with  $h = 2, 4, 8, 16, 32, 64,$  and  $128$  relative to the ferromagnetic energy as a function of  $J$ . Also shown is the energy of the antiferromagnetic phase (dotted line).

to a striped phase with increasingly larger width  $h$ . We also find that, for the range of values displayed in Fig. 2, the striped phase always exhibits a lower energy than the ferromagnetic phase.

On the basis of these numerical results, it is certainly plausible that extending the above calculation to higher order in  $h$  would reveal that the ferromagnetic phase does not stabilize for any finite value of  $J$ . The validity of such a conjecture cannot, however, be determined simply by extending the above calculations to higher and higher values of  $h$ , since the computational resources required for such a calculation rapidly become prohibitive. Instead an expression for the asymptotic form of  $E_{\text{dip}}(h)$  must be derived. Such an expression is presented in the following section.

#### IV. ANALYSIS OF THE STRIPED PHASE FOR LARGE $\Lambda$

To calculate the dipolar contribution to the ground-state energy of the striped phase in the limit  $\Lambda = 2ah \rightarrow \infty$ , from Eq. (8), we express the dipolar energy as

$$E = \int_{\Omega_B} d^2 Q \sigma(\vec{Q}) \sigma(-\vec{Q}) \Gamma(\vec{Q}), \quad (11)$$

where  $\sigma(\vec{Q})$  denotes the Fourier transform of the spin configuration  $\sigma(\vec{R})$ ,

$$\sigma(\vec{Q}) = \sum_{\vec{R}} e^{i\vec{Q}\cdot\vec{R}} \sigma(\vec{R}), \quad (12)$$

and we have defined  $\Gamma(\vec{Q})$  as

$$\Gamma(\vec{Q}) = \sum_{\vec{R}} \frac{e^{i\vec{Q}\cdot\vec{R}}}{R^3}. \quad (13)$$

The long-range character of the dipolar interaction manifests itself in the long-wavelength behavior of  $\Gamma(\vec{Q})$ , giving rise to a nonanalytic term proportional to  $Q$ ,<sup>12</sup>

$$\Gamma(\vec{Q}) = \Gamma_0 - 2\pi Q + \tilde{\Gamma}(\vec{Q}). \quad (14)$$

The presence of the linear term in  $\Gamma(\vec{Q})$  leads to a logarithmic contribution in the leading asymptotic correction to the dipolar energy of the striped phase, given by

$$\lim_{h \rightarrow \infty} E_{\text{dip}}(h) = E_{\text{dip}}^0 - \frac{1}{h} (A + B \ln h) + \mathcal{O}\left(\frac{1}{h^2}\right), \quad (15)$$

where  $E_{\text{dip}}^0$  denotes the dipolar energy of the ferromagnetic ground state and the parameters  $A$  and  $B$  are both positive constants. The detailed derivation of Eq. (15) is given in Appendix B, together with the explicit form of the coefficients  $A$  and  $B$ .  $B$  is evaluated exactly in Appendix B and  $A$  may be evaluated to give

$$A = 9.105 \quad (16)$$

and

$$B = 8. \quad (17)$$

[The value of  $A$  quoted here was obtained by fitting the asymptotic form to the data for large ( $h \geq 50$ ) but finite stripes described in the previous section.]

The above result implies that in the limit  $h \rightarrow \infty$  a plot of  $h[E_{\text{dip}}^0 - E_{\text{dip}}(h)]$  versus  $\ln h$  should be linear with slope  $A$  and  $y$  intercept  $B$ . Figure 3 shows such a plot calculated from the expression given by Eq. (A20) in Appendix A for selected values of  $h$  in the range  $h = 2-400$ , together with the result given by Eq. (15). It is seen that the above asymptotic approximation to the ground-state energy, given by Eq. (15), agrees well with the numerical results over a wide range of  $h$ .

Combining Eqs. (10) and (15), the ground-state energy of a striped phase of thickness  $h$  may be written as

$$\begin{aligned} \lim_{h \rightarrow \infty} E(h) &= E_{\text{dip}}(h) + E_{\text{ex}}(h) \\ &= E_F - \frac{1}{h} (A - 2J + B \ln h) + \mathcal{O}\left(\frac{1}{h^2}\right), \end{aligned} \quad (18)$$

where  $E_F \equiv E_{\text{dip}}^0 - 2J$  denotes the ground-state energy of the ferromagnetic state.

The equilibrium thickness of the striped phase for a given value of  $J$  may be found by differentiating Eq. (18)

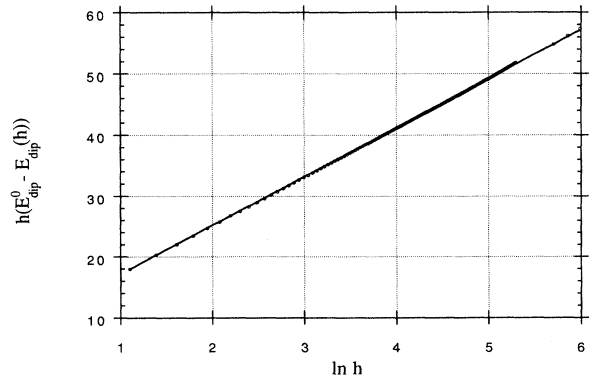


FIG. 3.  $\ln\{h[E_{\text{dip}}^0 - E_{\text{dip}}(h)]\}$  versus  $\ln h$  for the striped phase.

with respect to  $h$ . Referring to this equilibrium value as  $h^*$  one arrives at

$$B = A - 2J + B \ln h^*, \quad (19)$$

which leads to

$$\begin{aligned} h^* &= \exp \left[ 1 + \frac{2J - A}{B} \right] \\ &= h_0 \exp \left( \frac{J}{4} \right). \end{aligned} \quad (20)$$

In the above  $h_0 \equiv \exp(1 - \frac{A}{B}) = 0.871$ . Substituting the result for  $h^*$  back into Eq. (18) gives

$$\lim_{h \rightarrow \infty} E(h) = E_F - \frac{B}{h^*} + \mathcal{O} \left( \frac{1}{h^{*2}} \right). \quad (21)$$

This implies that the ferromagnetic phase is unstable in the thermodynamic limit for a two-dimensional spin system with a dipole-dipole and exchange interaction, since the phase with  $h = h^*$  will always have a lower energy. The origin of the instability is a direct consequence of logarithmic contribution in the asymptotic expansion of the dipolar energy of the striped phase, and hence may be attributed to the long-range character of the dipolar interaction in two dimensions.

The stability of the striped phase relative to the ferromagnetic phase and the exponential dependence of the stripe thickness  $h$  given by Eq. (20) are consistent with earlier work of Garel and Doniach,<sup>4</sup> using a phenomenological Ginzburg-Landau expression for the free energy, and the continuum model studied by Yafet and Gyorgy.<sup>5</sup> On the other hand Czech and Villain<sup>7</sup> have argued that for a uniaxial model the checkerboard phase has a lower energy than the striped phase. Kaplan and Gehring<sup>6</sup> have compared the energy of both the checkerboard phase and the striped phase within the framework of a continuum model of a uniaxial spin system and conclude that the striped phase has a lower free energy than the checkerboard phase. They attribute the discrepancy between their result and that of Czech and Villain to certain approximations introduced in their analysis.

The uncertainty surrounding the precise nature of the ground state arises from the fact that the energy of the checkerboard phase exhibits the same functional dependence on the characteristic dimension  $h$ , characterizing the size of the squares, as given by Eq. (15) for the striped phase. In particular the logarithmic contribution to the dipolar energy is independent of the particular phase and depends only on the the number of domain walls. As a consequence the difference in energy between the two phases is determined by the nonlogarithmic contributions to the dipolar energy, which are contained, to leading order, in the value of the coefficient  $B$ . Since these nonlogarithmic contributions depend sensitively on the structure and intersection of the domain walls, the precise value of the coefficient  $B$  depends on the model used and the approximations introduced in the subsequent analysis. In light of these considerations it is therefore worthwhile to extend the present analysis to the checkerboard phase described in Ref. 7 and to compare the results obtained

with the corresponding results for the striped phase.

The exchange energy for the checkerboard phase may be calculated from the Hamiltonian given by Eq. (9) as

$$E_{\text{ex}}(h) = -2J \left( 1 - \frac{2}{h} \right). \quad (22)$$

The dipolar contribution to the checkerboard phase may be evaluated numerically for a particular value of  $h$  from the expression given by Eq. (A26). Noting that the asymptotic form for the dipolar energy of the checkerboard configuration is that given in Eq. (15) above,<sup>7,6</sup> where  $h$  denotes the size of the squares, we plot  $\ln\{E_{\text{dip}}^0 - E_{\text{dip}}(h)\}$  versus  $\ln h$  in Fig. 4. The coefficients  $A$  and  $B$  may be evaluated to give

$$A = 2.819 \quad (23)$$

and

$$B = 16, \quad (24)$$

where the coefficient  $A$  was obtained by fitting the asymptotic form given by Eq. (15) to numerical results obtained from Eq. (A26) for large  $h$ . The resultant asymptotic form is shown by the solid line in Fig. 4. Minimizing the resultant form for the energy we obtain an equilibrium value of  $h = h^*$  identical to that given by Eq. (20), but with  $h_0 = \exp(1 - \frac{A}{B}) = 2.28$ .

The energies of the striped and checkerboard phases are compared in Fig. 5 and show that for a given value of  $J$  the striped phase has the lower energy. In the limit of large  $J$ , our analysis shows that the relevant quantity for determining the lower energy is not the value of  $B$ , as found in Ref. 7, but is instead the ratio  $B/h_0$  as shown in Ref. 6. This difference arises as a consequence of the fact that the second term contained in the expression of the dipolar energy given by Eq. (15) was omitted in the analysis given in Ref. 7. Since  $B/h_0 \approx 7.0$  for the checkerboard phase and  $B/h_0 \approx 9.2$  for the striped phase, we can conclude that the striped phase will always have the lower free energy. Thus, while our analysis of a microscopic model of a single layer of uniaxial spins on a square lattice differs somewhat from the continuum model of a thin film considered by Kaplan and Gehring<sup>6</sup> and, as a consequence, yields a different value for the coefficient  $A$  for both the striped phase and the checkerboard phase

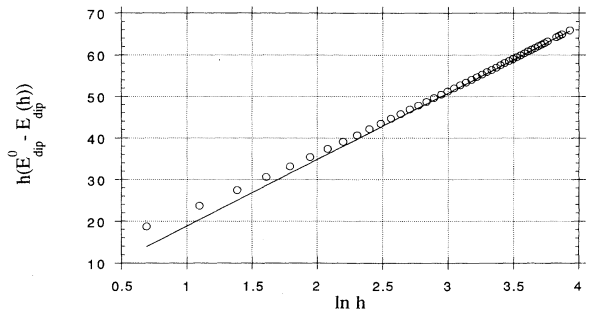


FIG. 4.  $\ln\{h[E_{\text{dip}}^0 - E_{\text{dip}}h]\}$  versus  $\ln h$  for the checkerboard phase.

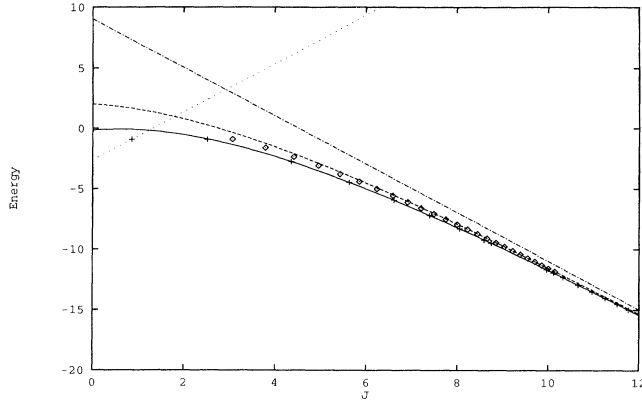


FIG. 5. Comparison of the energies of the striped and checkerboard phases. The solid line shows the asymptotic expression for the striped phase with the coefficients given in the text. The dashed line is the corresponding expression for the checkerboard phase. Crosses represent the points at which the width of the stripes change from  $h$  to  $h + 1$  (i.e., crossing points of the lowest energy lines in Fig. 3). Diamonds are the corresponding points for the checkerboard phases. For reference, the dot-dashed line and dotted line show the energies of the ferromagnetic and antiferromagnetic phases, respectively.

[in our analysis  $A = 4\pi b$  for the striped phase and  $4\pi b'$  for the corresponding checkerboard phase, where  $b$  and  $b'$  are defined in Eqs. (13) and (16) of Ref. 6], we nevertheless arrive at the same conclusion regarding their relative energies.

In order to get some feel for the size of the domains that might exist in a realistic system let us define the temperature  $T_c$ ,

$$k_B T_c = 2.269 J S_{\text{eff}}^2 \quad (25)$$

$$= 2.269 J \frac{\mu_{\text{eff}}^2}{2a^3}, \quad (26)$$

which corresponds to the critical temperature of our two-dimensional spin system in the absence of the dipolar interaction. We therefore obtain the following expression for the exponent  $J/B$ , which appears in Eq. (20):

$$\frac{2J}{B} = \frac{T_c}{T^*}, \quad (27)$$

where we have defined  $T^*$  as

$$T^* = 9.076 \frac{\mu_{\text{eff}}^2}{2k_B a^3}. \quad (28)$$

A more useful form of Eq. (28) is given by

$$T^* = 2.83 \frac{\mu_{\text{eff}}^2}{a^3} \text{ K}, \quad (29)$$

where  $T^*$  is expressed in kelvin, the effective moment  $\mu_{\text{eff}}$  is expressed in Bohr magnetons, and the lattice constant  $a$  in Å. If we consider by way of an example  $\text{Dy}^{3+}$ , with a ground-state doublet  $|\pm 15/2\rangle$ , with  $\mu_{\text{eff}} = 10.63\mu_B$  and  $a = 3.5 \text{ \AA}$ , then we obtain a value of  $T^* \approx 7.5 \text{ K}$ .

## V. PHASE DIAGRAM

The phase diagram for a temperature and exchange parameter phase space  $(T, J)$  was constructed using Monte Carlo simulations for a  $N = 16 \times 16$  system. The spin system was assumed to satisfy a periodic condition and the long-range nature of the dipolar interaction was treated using the Ewald summation technique.<sup>9</sup> A typical simulation included  $10^6$  Monte Carlo steps per spin to allow the system to reach equilibrium. This was followed by up to  $10^7$  more Monte Carlo steps per site, with data taken from every 10th configuration, except near the transition temperature where every 20th configuration was used. Temperatures are given in unit of  $\mu_{\text{eff}}^2/2a^3 k_B$ .

The phase boundaries between the striped phase and the disordered phase shown in Fig. 6 were determined from the peak in the calculation of the specific heat. In the calculation of the specific heat it was found that for small values of the exchange parameter, if one starts at a high temperature in a random state and then very slowly cools the system, domain walls form at high temperatures which persist for long times at lower temperatures. The long life of these domain walls may be attributed to the ground-state energies of the striped phase being only slightly larger than that of the antiferromagnetic ground state. While the presence and the motion of these domain walls will involve little cost in energy, they nevertheless cause large fluctuations in the order parameter and hence an unusually large susceptibility. Domain wall formation can, therefore, make results from Monte Carlo simulations of uniaxial dipolar systems very difficult to decipher. For this reason simulations were either started from the expected ground state or from the final state from a previous simulation at a lower temperature. The resultant phase boundaries are shown as diamonds in Fig. 6.

The phase boundaries separating the various striped phases were also determined from Monte Carlo simulations by considering the system at constant  $T < T_c$  and varying the strength of the exchange coupling. The transformation of the system from one striped phase to

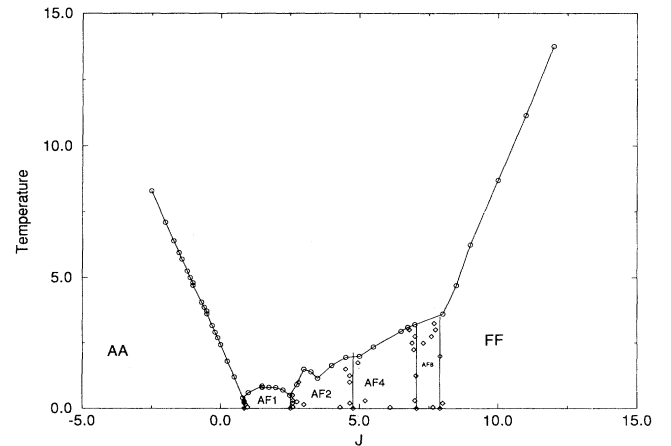


FIG. 6. Phase diagram for a  $N = 16 \times 16$  system from Monte Carlo simulations.

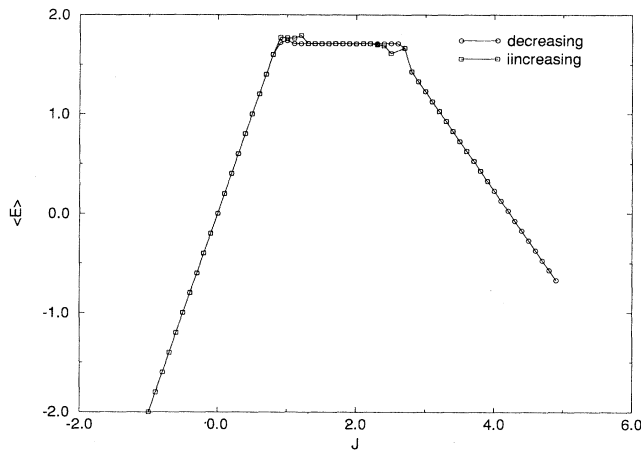


FIG. 7. Average internal energy versus  $J$  from a Monte Carlo simulation on a  $N = 16 \times 16$  system.

another gives rise to a discontinuous change in the slope of the average internal energy of the system with increasing or decreasing  $J$ . In Fig. 7 this discontinuity, at the transition from antiferromagnetic to the  $h = 1$  phase and then to the  $h = 2$  phase, is clearly observable, both for increasing and decreasing  $J$ . The determination of the phase boundaries separating the various striped phases is complicated, however, by two factors, namely, finite-size effects and hysteresis. From Fig. 7 it is seen that the effects of hysteresis are relatively minor. However, because of the finite size of the lattice, only those phases with a modulation commensurate with the assumed periodic nature of the spin system are observed. This means that while the AF2 and the AF4 phases are observed, the AF3 phase ( $h = 3$ ) is not observed. While this problem may be overcome by going to larger lattice sizes, the phase diagram given in Fig. 6 nevertheless provides a qualitative description of the phase boundaries in an infinite system, at least for small values of  $J$ .

It is important to note that the Monte Carlo simulations showed no evidence of ordering in a checkerboard state. Any tendency to form a checkerboard state would be seen in the structure factor discussed in Sec. VI.

## VI. STRUCTURE FACTOR

A particularly useful quantity when dealing with many different ordered phases is the structure factor defined by<sup>13</sup>

$$S(\vec{K}) = \left\langle \left| \sum_{\vec{r}} S(\vec{r}) e^{i\vec{K} \cdot \vec{r}} \right|^2 \right\rangle. \quad (30)$$

A pictorial representation of the structure factor intensity may, in principle, be compared directly with diffraction patterns determined experimentally. The intensity of a diffraction spot peculiar to a given ordered phase provides an order parameter for that phase. In this work the structure factor represented as a diffraction pattern generated during the simulation has been used to distinguish

the striped phases and to identify the phase boundaries between them. Figure 8 shows the diffraction patterns calculated for a system with  $J = 5.5$ , which places it in the AF4 phase. The peaks at  $\vec{K} = (0, \pm \frac{\pi}{4})$  and  $\vec{K} = (0, \pm \frac{3\pi}{4})$  are characteristic of the AF4 phase. Figure 9 is a plot of the magnitude of the  $(0, \frac{\pi}{4})$  peaks of Fig. 8 as a function of temperature. This gives an estimate of the Néel temperature of  $2.6 \pm 0.1$ , in agreement with that taken from the specific heat. A similar analysis has been done for

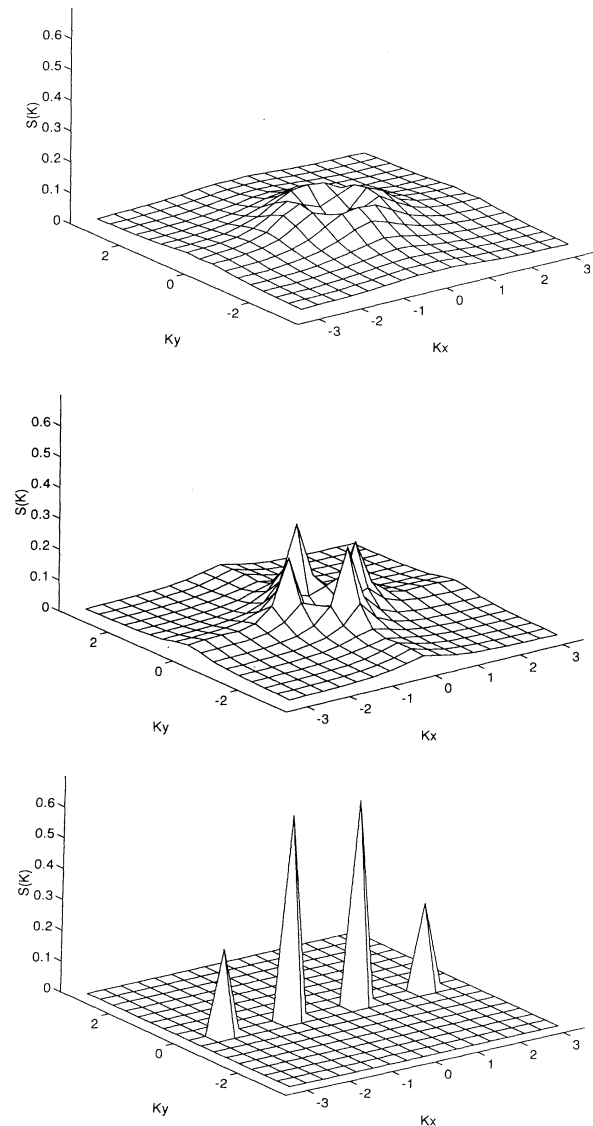


FIG. 8. Structure factor for a  $N = 16 \times 16$  (a) above  $T_c$  ( $T = 5.00$ ), (b) near  $T_c$  ( $T = 3.00$ ), and (c) below  $T_c$  ( $T = 0.50$ ) for  $J = 5.5$ . The peaks at  $(0, \pm \pi/4)$  and  $(0, \pm 3\pi/4)$  are characteristic of the AF4 phase. Note that just above  $T_c$  ( $T = 3.00$ ) four small peaks form, indicating the presence of both regions of the AF4 phase and regions of the FA4 phase (i.e., the AF4 phase rotated by  $90^\circ$ ). Note also the existence of some small residual structure, indicating residual ordering on short scales, well above  $T_c$  ( $T = 5.00$ ).

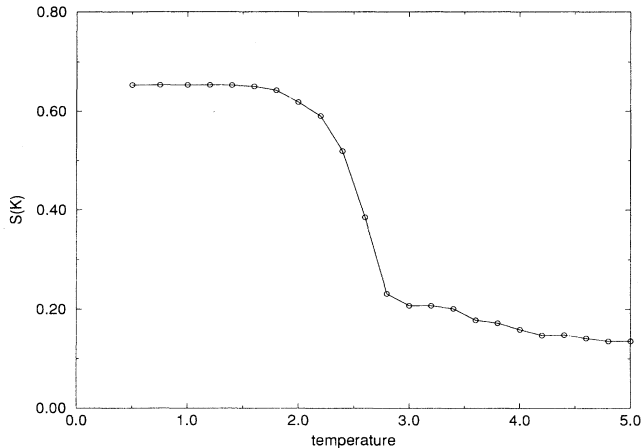


FIG. 9. Magnitude of the principal structure factor peaks [ $\vec{K} = (0, \pm \frac{\pi}{4})$ ] of Fig. 8.

other values of the exchange parameter to help in determining both the ground state and the Néel temperature.

## VII. CONCLUSION

We have obtained an analytic expression for the ground-state energy for the striped phase of a two-dimensional uniaxial dipolar spin system in the limit  $h \rightarrow \infty$ . The resultant expression is found to be in excellent agreement with earlier numerical results<sup>1,2</sup> and provides an excellent approximation to the exact expression, even for relatively small values of the modulation length ( $h \approx 8$ ). Based on this result we have shown that the dipolar interaction will always destabilize the ferromagnetic state regardless of the strength of the exchange coupling, and that the ground state will instead consist of an antiferromagnetic superlattice similar to that shown schematically in Fig. 1, with a modulation length that depends exponentially on the strength of the exchange coupling according to Eq. (20). The analysis shows that the appearance of the modulated spin phase may be attributed to the nonanalytic nature of the dipolar interaction in the long-wavelength limit. Specifically it is due to the term proportional to the magnitude of the wave number  $Q$  in Eq. (14), which arises as a consequence of the long-range nature of the dipolar interaction. Earlier work on continuum models,<sup>5,4</sup> that deals with a somewhat different limit of the thin magnetic films also concludes that striped phases will always be stable with respect to the ferromagnetic state.

We have also shown that while the striped phase has a lower energy than the corresponding checkerboard phase for a given value of  $J$ , the values are very close. This arises as a consequence of the fact that for a given number of domain walls the difference in energy between the two phases is determined by the corrections to the logarithmic contributions to the dipolar energy. This result, together with the fact that these corrections depend sensitively on the structure and intersection of the domain walls,

accounts for the quantitative differences between the results obtained in the lattice and continuum models. (For further discussion of the relationship between the continuum approximation, experimental systems, and the present work see Ref. 14.) It is interesting to note, however, that despite these differences, the ground state, in both cases, is the striped phase.

We have also extended the results to finite temperature by means of Monte Carlo simulations and obtained the phase diagram for a finite  $16 \times 16$  lattice. This provides at least a qualitative description of the infinite-size system. However, the extension of the results on the finite lattice to an infinite system is complicated by the fact that certain phases, not commensurate with the dimensions of the lattice, are not observed due to finite-size effects.

The magnetic phases discussed in the present analysis pose a number of intriguing problems. The most obvious questions concern the extension of these results to finite temperature. Our finite-temperature Monte Carlo calculations are consistent with the ground-state energy calculations in that the ordered phases are striped phases and the checkerboard phases are not observed. At finite temperature domain wall roughening<sup>15</sup> should begin to play an important role and one might expect the domain walls to acquire a finite curvature particularly for large values of modulation length  $\Lambda$ . Recently Kashuba and Pokrovsky<sup>16</sup> have considered domain wall formation at a finite temperature based on a continuum model of a two-dimensional dipolar system. One might also wonder about the effect of defects on the properties of the striped phase. Finally the distinct character of the dipolar interaction in two and three dimensions suggests that the generalization of these studies to systems composed of several layers would provide an interesting and important extension of this work.

## ACKNOWLEDGMENTS

This work was supported in part by the Natural Sciences and Engineering Council of Canada (NSERC). One of the authors (A.B.M.I.) would like to thank Dr. Hans Herrmann and the HLRZ, Jülich, Germany for the hospitality during his stay. Some of the Monte Carlo work was carried out on the Fujitsu VPX240 at the High Performance Computing Centre (HPCC) in Calgary, Canada.

## APPENDIX A

In this appendix we will calculate the energy of a striped phase of thickness  $h$  as given in Eq. (8). The energy of such a phase is given by

$$E = \sum_{n \neq m} \frac{\sigma_m \sigma_n}{R_{mn}^3}, \quad (\text{A1})$$

where  $R_{mn}$  is defined in Eq. (6). The striped phases are translationally invariant along the  $y$  direction and are periodic with modulation length  $\Lambda = 2ha$  in the  $x$  direction. A schematic representation of the striped phase

with  $h = 4$  is given in Fig. 1. Given the symmetry of the striped phases we may replace the sum over all spins  $n$  by a sum over the spins in a single strip of width  $h$  and a sum over all superlattice vectors  $\vec{G}$  of the striped phase:

$$E = \sum'_m \sum_{n=1}^h \sum_{\vec{G}} \frac{\sigma_{n+g_1} \sigma_m}{|\vec{r}_{mn} + \vec{G}|^3}, \quad (\text{A2})$$

where the vector  $\vec{r}_{mn} = (m - n, 0)$  and is confined to a single strip. The prime on the sum over  $m$  reminds us that we exclude the case when  $m$  and  $n$  refer to the same spin (when  $m = n$  and  $|\vec{G}| = 0$ ). Given the periodicity of the square lattice, as well as the symmetry of the striped phases we have defined,

$$\vec{G} = (g_1 h, g_2), \quad (\text{A3})$$

$$\sigma_m = -\sigma_{m+h}, \quad (\text{A4})$$

with  $\sigma_1 \equiv 1$ .

Our system will be made up of  $\frac{N}{h}$  equivalent sites, where  $N$  is the total number of spins in the system. Equation (A2) may then be written as

$$E = \frac{N}{h} \sum_{m=1}^h \sum_{n=1}^h \sum'_{\vec{G}} \frac{\sigma_{n+g_1} \sigma_m}{|\vec{r}_{mn} + \vec{G}|^3}. \quad (\text{A5})$$

Equation (A5) naturally breaks into two parts. The first part contains the interaction between spins which occupy equivalent positions in the  $y$  direction in equivalent stripes. The second part contains all other interactions. Therefore we may write

$$E = \frac{N}{h} \left( h \sum_{\vec{G} \neq 0} \frac{(-1)^{g_1}}{|\vec{G}|^3} + \sum_{m=1}^h \sum_{n=1}^h \sum'_{\vec{G}} \frac{(-1)^{g_1}}{|\vec{r}_{mn} + \vec{G}|^3} \right), \quad (\text{A6})$$

where the prime means that the term  $m = n$  is excluded from the sum.

The evaluation of the terms appearing in the above expression is complicated by the long-range character of the dipolar interaction and is best accomplished by a variation of the Ewald summation technique described in earlier work.<sup>10,11</sup> This allows us to express the above summation in terms of a combination of rapidly convergent series.

Let us consider the second of the two terms that appear in Eq. (A6). In order to evaluate this sum we use the integral representation

$$\frac{1}{R^3} = \frac{4}{\sqrt{\pi}} \int_0^\infty d\rho \rho^2 e^{-R^2 \rho^2} \quad (\text{A7})$$

and write the sum in two parts as

$$\begin{aligned} \sum_{\vec{G}} \frac{(-1)^{g_1}}{|\vec{r}_{mn} + \vec{G}|^3} &= \sum_{\vec{G}} (-1)^{g_1} \frac{4}{\sqrt{\pi}} \int_0^\infty d\rho \rho^2 e^{-|\vec{r}_{mn} + \vec{G}|^2 \rho^2} \\ &= \sum_{\vec{G}} (-1)^{g_1} \frac{4}{\sqrt{\pi}} \left( \int_0^\eta d\rho \rho^2 e^{-|\vec{r}_{mn} + \vec{G}|^2 \rho^2} \right. \\ &\quad \left. + \int_\eta^\infty d\rho \rho^2 e^{-|\vec{r}_{mn} + \vec{G}|^2 \rho^2} \right). \quad (\text{A8}) \end{aligned}$$

The second integral appearing in Eq. (A8) may be readily evaluated as

$$\int_\eta^\infty d\rho \rho^2 e^{-|\vec{r}_{mn} + \vec{G}|^2 \rho^2} = \frac{F_1(\eta |\vec{r}_{mn} + \vec{G}|)}{|\vec{r}_{mn} + \vec{G}|^3}, \quad (\text{A9})$$

where  $F_1(x)$  is given by

$$F_1(x) = \frac{1}{2} x e^{-x^2} + \frac{\sqrt{\pi}}{4} \operatorname{erfc}(x), \quad (\text{A10})$$

to yield a rapidly convergent series

$$\begin{aligned} \sum_{\vec{G}} (-1)^{g_1} \frac{4}{\sqrt{\pi}} \int_\eta^\infty d\rho \rho^2 e^{-|\vec{r}_{mn} + \vec{G}|^2 \rho^2} \\ = \frac{4}{\sqrt{\pi}} \sum_{\vec{G}} (-1)^{g_1} \frac{F_1(\eta |\vec{r}_{mn} + \vec{G}|)}{|\vec{r}_{mn} + \vec{G}|^3}. \quad (\text{A11}) \end{aligned}$$

The first sum appearing in Eq. (A8) may also be made rapidly convergent by converting the sum over superlattice vectors to a sum over the corresponding reciprocal lattice vectors to give

$$\begin{aligned} \sum_{\vec{G}} (-1)^{g_1} \frac{4}{\sqrt{\pi}} \int_0^\eta d\rho \rho^2 e^{-|\vec{r}_{mn} + \vec{G}|^2 \rho^2} \\ = \frac{4\sqrt{\pi}}{h} \sum_{\vec{Q}} e^{i\vec{Q} \cdot \vec{r}_{mn}} \int_{\frac{1}{h}}^\infty \frac{d\rho}{\rho^2} e^{-\rho^2 |\vec{Q}|^2 / 4} \\ = \frac{4\sqrt{\pi}}{h} \sum_{\vec{Q}} \frac{|\vec{Q}|}{2} F_2\left(\frac{|\vec{Q}|}{2\eta}\right) e^{i\vec{Q} \cdot \vec{r}_{mn}}, \quad (\text{A12}) \end{aligned}$$

where we have defined  $F_2(x)$  as

$$F_2(x) = \frac{e^{-x^2}}{x} - \sqrt{\pi} \operatorname{erfc}(x) \quad (\text{A13})$$

and we have defined the vector  $\{\vec{Q}\}$  as

$$\vec{Q} = 2\pi \left( \frac{l_1 - 1/2}{h}, l_2 \right), \quad (\text{A14})$$

where  $l_1$  and  $l_2$  are integers.

The first term appearing in Eq. (A6) may be evaluated in a similar manner,

$$\begin{aligned} \sum_{\vec{G} \neq 0} \frac{(-1)^{g_1}}{|\vec{G}|^3} &= \sum_{\vec{G} \neq 0} (-1)^{g_1} \frac{4}{\sqrt{\pi}} \int_0^\infty d\rho \rho^2 e^{-|\vec{G}|^2 \rho^2} \\ &= \sum_{\vec{G} \neq 0} (-1)^{g_1} \frac{4}{\sqrt{\pi}} \left( \int_0^\eta d\rho \rho^2 e^{-|\vec{G}|^2 \rho^2} \right. \\ &\quad \left. + \int_\eta^\infty d\rho \rho^2 e^{-|\vec{G}|^2 \rho^2} \right), \quad (\text{A15}) \end{aligned}$$

where, as in the previous case, we have divided the integral into two parts to improve the convergence properties of the summation.

The second term in Eq. (A15) may be readily evaluated to give

$$\begin{aligned} \sum_{\vec{G} \neq 0} \frac{(-1)^{g_1} 4}{\sqrt{\pi}} \int_{\eta}^{\infty} d\rho \rho^2 e^{-|\vec{G}|^2 \rho^2} \\ = \frac{4}{\sqrt{\pi}} \sum_{\vec{G} \neq 0} (-1)^{g_1} \frac{F_1(\eta|\vec{G}|)}{|\vec{G}|^3}, \end{aligned} \quad (\text{A16})$$

where the function  $F_1(x)$  was defined earlier by Eq. (A10). The first term in Eq. (A15) may be evaluated by transforming the sum over lattice vectors to one over reciprocal lattice vectors to give

$$\begin{aligned} \sum_{\vec{G} \neq 0} (-1)^{g_1} \frac{4}{\sqrt{\pi}} \int_0^{\eta} d\rho \rho^2 e^{-|\vec{G}|^2 \rho^2} \\ = \frac{4}{\sqrt{\pi}} \left[ \frac{\pi}{h} \sum_{\vec{Q}} \int_{\frac{1}{\eta}}^{\infty} \frac{d\rho}{\rho^2} e^{-\rho^2 |\vec{Q}|^2 / 4} - \frac{\eta^3}{3} \right], \end{aligned} \quad (\text{A17})$$

where the reciprocal lattice vector  $\vec{Q}$  is given by

$$\vec{Q} = 2\pi \left( \frac{l_1 - 1/2}{h}, l_2 \right). \quad (\text{A18})$$

This integral may be readily evaluated to give

$$\begin{aligned} \sum_{\vec{G} \neq 0} (-1)^{g_1} \frac{4}{\sqrt{\pi}} \int_0^{\eta} d\rho \rho^2 e^{-|\vec{G}|^2 \rho^2} \\ = \frac{4}{\sqrt{\pi}} \left[ \frac{\pi}{h} \sum_{\vec{Q}} \frac{|\vec{Q}|}{2} F_2 \left( \frac{|\vec{Q}|}{2\eta} \right) - \frac{\eta^3}{3} \right]. \end{aligned} \quad (\text{A19})$$

Thus combining terms we have that

$$\begin{aligned} \frac{E}{N} = \frac{4}{\sqrt{\pi}} \left( \sum_{\vec{G} \neq 0} (-1)^{g_1} \frac{F_1(\eta|\vec{G}|)}{|\vec{G}|^3} + \frac{1}{h} \sum_{\vec{G}} \sum_{m=1}^h \sum_{n=1}^h ' (-1)^{g_1} \frac{F_1(\eta|\vec{r}_{mn} + \vec{G}|)}{|\vec{r}_{mn} + \vec{G}|^3} \right) \\ + \frac{4\sqrt{\pi}}{h} \sum_{\vec{Q}} \frac{|\vec{Q}|}{2} F_2 \left( \frac{|\vec{Q}|}{2\eta} \right) \left( 1 + \frac{1}{h} \sum_{m=1}^h \sum_{n=1}^h ' e^{i\vec{Q} \cdot \vec{r}_{mn}} \right) - \frac{4\eta^3}{3\sqrt{\pi}}. \end{aligned} \quad (\text{A20})$$

We may carry out a similar calculation for the checkerboard phases. We begin equivalently with Eq. (A1), with  $R_{mn}$  defined as before. The system now possesses periodicity in both the  $x$  and  $y$  directions with a modulation length  $\Lambda = 2ha$ . We may therefore replace the sum over all spins  $n$  by a sum over all spins in a single square of size  $h \times h$  and a sum over all superlattice vectors  $\vec{G}$ :

$$E = \sum_m ' \sum_{n=1}^{h^2} \sum_{\vec{G}} \frac{\sigma(\vec{r}_n + \vec{G}) \sigma(\vec{r}_m)}{|\vec{r}_{mn} + \vec{G}|^3}. \quad (\text{A21})$$

Here the vector  $\vec{r}_{nm}$  is confined to lie in the single square of spins. For the checkerboard phases the superlattice vector  $\vec{G}$  is defined as

$$\vec{G} = (g_1 h, g_2 h) \quad (\text{A22})$$

and the symmetry of the system is such that

$$\sigma(\vec{r}) = (-1)^{g_1 + g_2} \sigma(\vec{r} + \vec{G}). \quad (\text{A23})$$

The system is now made up of  $\frac{N}{h^2}$  equivalent sites and we may write Eq. (A21) as

$$E = \frac{N}{h^2} \sum_{m=1}^{h^2} \sum_{n=1}^{h^2} ' \sum_{\vec{G}} \frac{\sigma(\vec{r}_n + \vec{G}) \sigma(\vec{r}_m)}{|\vec{r}_{mn} + \vec{G}|^3}, \quad (\text{A24})$$

which, using Eq. (A23), may be written as

$$\begin{aligned} E = \frac{N}{h^2} \left( h^2 \sum_{\vec{G} \neq 0} \frac{(-1)^{g_1 + g_2}}{|\vec{G}|^3} \right. \\ \left. + \sum_{m=1}^{h^2} \sum_{n=1}^{h^2} ' \sum_{\vec{G}} \frac{(-1)^{g_1 + g_2}}{|\vec{r}_{mn} + \vec{G}|^3} \right), \end{aligned} \quad (\text{A25})$$

where the prime means that the term  $m = n$  is excluded from the sum. The calculation proceeds exactly as for the striped phases and hence we quote here only the conclusion:

$$\begin{aligned} \frac{E}{N} = \frac{4}{\sqrt{\pi}} \left( \sum_{\vec{G} \neq 0} (-1)^{g_1 + g_2} \frac{F_1(\eta|\vec{G}|)}{|\vec{G}|^3} + \frac{1}{h^2} \sum_{\vec{G}} \sum_{m=1}^{h^2} \sum_{n=1}^{h^2} ' (-1)^{g_1 + g_2} \frac{F_1(\eta|\vec{r}_{mn} + \vec{G}|)}{|\vec{r}_{mn} + \vec{G}|^3} \right) \\ + \frac{4\sqrt{\pi}}{h^2} \sum_{\vec{Q}} \frac{|\vec{Q}|}{2} F_2 \left( \frac{|\vec{Q}|}{2\eta} \right) \left( 1 + \frac{1}{h^2} \sum_{m=1}^{h^2} \sum_{n=1}^{h^2} ' e^{i\vec{Q} \cdot \vec{r}_{mn}} \right) - \frac{4\eta^3}{3\sqrt{\pi}}. \end{aligned} \quad (\text{A26})$$

In this result we have retained the definitions of the functions  $F_1$  and  $F_2$  from the striped phase calculation, but have redefined the vectors  $\vec{G}$ , as given in Eq. (A22) and  $\vec{Q}$  as

$$\vec{Q} = 2\pi \left( \frac{l_1 - 1/2}{h}, \frac{l_2 - 1/2}{h} \right). \quad (\text{A27})$$

## APPENDIX B

In this appendix we present the derivation of dipolar energy of the striped phase in the limit  $\Lambda = 2ah \rightarrow \infty$  given by Eq. (15). The initial part of the analysis is similar in many respects to that presented in Appendix A. We begin with the expression for the dipolar energy given by Eq. (8),

$$E = \sum_{i \neq j} \frac{\sigma_i \sigma_j}{R_{ij}^3}, \quad (\text{B1})$$

where  $R_{ij}$  is defined by Eq. (6) and denotes the distance between the lattice sites  $i$  and  $j$  in units of the lattice constant. We express the lattice vector  $\vec{R}$  in terms of the  $x$  and  $y$  coordinates  $m$  and  $n$  as

$$\vec{R} = (m, n). \quad (\text{B2})$$

In the striped phase the spin configuration  $\sigma(\vec{R}_i)$  is translationally invariant along the  $y$  direction ( $n$  direction) and is periodic with modulation length  $\Lambda = 2ha$  in the  $x$  direction ( $m$  direction). A schematic representation of the striped phase for  $h = 4$  is shown in Fig. 1. The symmetry of the striped phase means that we can write the spin at lattice vector  $\vec{R}$  as

$$\sigma(\vec{R}) = \sigma_m, \quad (\text{B3})$$

where  $\sigma_m$  is defined such that

$$\sigma_m = -\sigma_{m+h}, \quad (\text{B4})$$

with  $\sigma_1 = 1$ .

We define the Fourier transform of the spin configuration  $\sigma(\vec{R})$  as

$$\sigma(\vec{R}) = \int_{\Omega_B} d^2Q e^{i\vec{Q} \cdot \vec{R}} \sigma(\vec{Q}), \quad (\text{B5})$$

where  $\Omega_B$  denotes the first Brillouin zone. We have therefore

$$\sigma(\vec{Q}) = \frac{1}{(2\pi)^2} \sum_{\vec{R}} \sigma(\vec{R}) e^{-i\vec{Q} \cdot \vec{R}}. \quad (\text{B6})$$

The Fourier transformation of the spin configuration,  $\sigma(\vec{Q})$ , may be calculated explicitly as

$$\begin{aligned} \sigma(\vec{Q}) &= \frac{1}{(2\pi)^2} \sum_n e^{-iQ_y n} \sum_m e^{-iQ_x m} \sigma_m \\ &= \frac{1}{h} \delta(Q_y) \sum_m F(K_m) \delta(Q_x - K_m), \end{aligned} \quad (\text{B7})$$

where  $K_m$  and  $F(K_m)$  are defined as

$$K_m = \frac{2\pi}{h} \left( m + \frac{1}{2} \right) \quad (\text{B8})$$

$$F(x) = \frac{2e^{-ix}}{1 - e^{-ix}}, \quad (\text{B9})$$

respectively. Substituting this into our expression for the dipolar energy, we obtain

$$\begin{aligned} E &= \int_{\Omega_b} d^2Q_1 \int_{\Omega_b} d^2Q_2 \sigma(\vec{Q}_1) \sigma(\vec{Q}_2) \\ &\times \sum_{\vec{R}_1 \neq \vec{R}_2} \frac{e^{i(\vec{Q}_1 \cdot \vec{R}_1 + \vec{Q}_2 \cdot \vec{R}_2)}}{|\vec{R}_1 - \vec{R}_2|^3}, \end{aligned} \quad (\text{B10})$$

which, after some algebra, reduces to

$$E = \int_{\Omega_B} d^2Q \sigma(\vec{Q}) \sigma(-\vec{Q}) \Gamma(\vec{Q}), \quad (\text{B11})$$

where we have defined  $\Gamma(\vec{Q})$  as

$$\Gamma(\vec{Q}) = \sum_{\vec{R}} \frac{e^{i\vec{Q} \cdot \vec{R}}}{|\vec{R}|^3}. \quad (\text{B12})$$

Substituting the explicit form for  $\sigma(\vec{Q})$  given by Eq. (B7), we obtain

$$E = \frac{N^2}{h^2} \sum_{m=-\frac{(h+1)}{2}}^{\frac{(h-1)}{2}} |F(K_m)|^2 \Gamma(K_m). \quad (\text{B13})$$

It may be readily shown that

$$|F(K_m)|^2 = \frac{1}{\sin^2\left(\frac{K_m}{2}\right)}. \quad (\text{B14})$$

Thus

$$\begin{aligned} \frac{E}{N^2} &= \frac{1}{h^2} \sum_{m=-\frac{(h+1)}{2}}^{\frac{(h-1)}{2}} \frac{\Gamma(K_m)}{\sin^2\left(\frac{K_m}{2}\right)} \\ &= \frac{2}{h^2} \left[ \sum_{n=0}^{\frac{(h-1)}{2}} \frac{\Gamma\left[\frac{2\pi}{h}\left(n + \frac{1}{2}\right)\right]}{\sin^2\left[\frac{\pi}{h}\left(n + \frac{1}{2}\right)\right]} \right]. \end{aligned} \quad (\text{B15})$$

As in the calculation presented in Appendix A, the calculation of  $\Gamma(K_m)$  is complicated by the long-range character of the dipolar interaction, and is best accomplished by a variation of the Ewald summation technique described in earlier work.<sup>10,11</sup> This not only provides an efficient basis for the numerical evaluation of  $\Gamma(Q)$  but also allows us to extract an analytical expression for the long-wavelength behavior, which, we will show, determines the dominant contribution to the dipolar energy of the striped phase for large  $h$ . We begin by noting that

$$\Gamma(\vec{Q}) = \sum_{\vec{R} \neq 0} \frac{e^{i\vec{Q} \cdot \vec{R}}}{|\vec{R}|^3} \quad (\text{B16})$$

$$= \frac{4}{\sqrt{\pi}} \sum_{\vec{R} \neq 0} \int_0^\infty d\rho \rho^2 e^{-R^2 \rho^2} e^{i\vec{Q} \cdot \vec{R}}. \quad (\text{B17})$$

We then separate the integral over  $\rho$  in terms of an integral from 0 to  $\eta$  and from  $\eta$  to  $\infty$  to give

$$\Gamma(\vec{Q}) = \frac{4}{\sqrt{\pi}} \sum_{\vec{R} \neq 0} \left( \int_0^\eta d\rho \rho^2 e^{-R^2 \rho^2} e^{i\vec{Q} \cdot \vec{R}} + \int_\eta^\infty d\rho \rho^2 e^{-R^2 \rho^2} e^{i\vec{Q} \cdot \vec{R}} \right). \quad (\text{B18})$$

Denoting the first term by  $B_3(\vec{Q}, \eta)$ , we obtain

$$\begin{aligned} B_3(\vec{Q}, \eta) &= \sum_{\vec{R} \neq 0} \int_\eta^\infty \rho^2 d\rho e^{-R^2 \rho^2} e^{i\vec{Q} \cdot \vec{R}} \\ &= \sum_{\vec{R} \neq 0} F_1(\eta|\vec{R}|) \frac{e^{i\vec{Q} \cdot \vec{R}}}{|\vec{R}|^3}. \end{aligned} \quad (\text{B19})$$

We have defined the function  $F_1(x)$  in Eq. (A10).

The form of  $B_3(\vec{Q})$  allows us to write

$$B_3(\vec{Q}) = B_3(0) + \tilde{B}_3(\vec{Q}), \quad (\text{B20})$$

where  $\tilde{B}_3(\vec{Q})$  is defined such that in the long-wavelength limit

$$\lim_{Q \rightarrow 0} \tilde{B}_3(\vec{Q}) \approx D_3 Q^2 + \dots \quad (\text{B21})$$

For the second term in Eq. (B18), we find it convenient to convert the expression to a summation in reciprocal lattice space. Defining the reciprocal lattice vector  $\vec{G}$  as

$$\vec{G} = 2\pi(g_1, g_2), \quad g_1, g_2 = 0, \pm 1, \pm 2, \dots, \quad (\text{B22})$$

we obtain after some algebra

$$\begin{aligned} \frac{4}{\sqrt{\pi}} \sum_{\vec{R} \neq 0} \int_0^\eta d\rho \rho^2 e^{-R^2 \rho^2} e^{i\vec{Q} \cdot \vec{R}} &= -\frac{4}{\sqrt{\pi}} \int_0^\eta \rho^2 d\rho + 4\sqrt{\pi} \int_0^\eta d\rho e^{-\frac{|\vec{Q}|^2}{4\rho^2}} + 4\sqrt{\pi} \sum_{\vec{G} \neq 0} \int_0^\eta d\rho e^{-\frac{|\vec{Q} + \vec{G}|^2}{4\rho^2}} \\ &= \frac{4}{\sqrt{\pi}} \left[ -\frac{\eta^3}{3} + \pi \frac{|\vec{Q}|}{2} F_2\left(\frac{|\vec{Q}|}{2\eta}\right) + \pi \sum_{\vec{G} \neq 0} \frac{|\vec{Q} + \vec{G}|}{2} F_2\left(\frac{|\vec{Q} + \vec{G}|}{2\eta}\right) \right], \end{aligned} \quad (\text{B23})$$

with  $F_2(x)$  defined by Eq. (A12).

We separate out the nonanalytic part of long-wavelength behavior of this contribution by writing the function  $\tilde{Q} F_2(|\vec{Q}|/2\eta)$  as

$$\frac{\pi|\vec{Q}|}{2} F_2\left(\frac{|\vec{Q}|}{2\eta}\right) = \pi\eta - \frac{\pi^3}{2} |\vec{Q}| + \tilde{B}_0(\vec{Q}), \quad (\text{B24})$$

with  $\tilde{B}_0(\vec{Q})$  defined such that

$$\lim_{Q \rightarrow 0} \tilde{B}_0(\vec{Q}) \approx D_0 Q^2 + \dots \quad (\text{B25})$$

Similarly we may write

$$\pi \sum_{\vec{G} \neq 0} |\vec{Q} + \vec{G}| F_2\left(\frac{|\vec{Q} + \vec{G}|}{2\eta}\right) = B_1(0) + \tilde{B}_1(\vec{Q}), \quad (\text{B26})$$

where  $\tilde{B}_1(\vec{Q})$  is defined such that

$$\lim_{Q \rightarrow 0} \tilde{B}_1(\vec{Q}) \approx D_1 Q^2 + \dots \quad (\text{B27})$$

Combining terms we obtain

$$\begin{aligned} \Gamma(K_m) &= \frac{4}{\sqrt{\pi}} \left( B_3(0) - \frac{\eta^3}{3} + \pi\eta + B_1(0) \right) \\ &\quad - 2\pi K_m + \frac{4}{\sqrt{\pi}} \\ &\quad \times \left[ \tilde{B}_3(K_m) + \tilde{B}_0(K_m) + \tilde{B}_1(K_m) \right] \end{aligned} \quad (\text{B28})$$

$$= \left[ \Gamma_0 - 2\pi K + \tilde{\Gamma}(K_m) \right], \quad (\text{B29})$$

with  $\Gamma_0$  and  $\tilde{\Gamma}(K_m)$  defined as

$$\Gamma_0 = \frac{4}{\sqrt{\pi}} \left[ B_3(0) + B_1(0) + \pi\eta \left( 1 - \frac{\eta^2}{3\pi} \right) \right] \quad (\text{B30})$$

and

$$\tilde{\Gamma}(K_m) = \frac{4}{\sqrt{\pi}} \left[ \tilde{B}_0(K_m) + \tilde{B}_1(K_m) + \tilde{B}_3(K_m) \right], \quad (\text{B31})$$

respectively. We note that  $\tilde{\Gamma}(K_m)$  is defined such that

$$\lim_{K_m \rightarrow 0} \tilde{\Gamma}(K_m) \approx DK_m^2 + \dots \quad (\text{B32})$$

Substituting the result for  $\Gamma(K_m)$  into the expression for the dipolar energy of the striped phase given

by Eq. (B13), we obtain that

$$\frac{E}{N^2} = \frac{E_0}{N^2} + \frac{E_1}{N^2} + \frac{E_3}{N^2}, \quad (\text{B33})$$

where we have defined

$$\frac{E_0}{N^2} = \frac{2\Gamma_0}{h^2} \sum_{n=0}^{\frac{h-1}{2}} \frac{1}{\sin^2 \left[ \frac{\pi}{h} \left( n + \frac{1}{2} \right) \right]}, \quad (\text{B34})$$

$$\frac{E_1}{N^2} = -\frac{8\pi^2}{h^3} \sum_{n=0}^{\frac{h-1}{2}} \frac{\left( n + \frac{1}{2} \right)}{\sin^2 \left[ \frac{\pi}{h} \left( n + \frac{1}{2} \right) \right]}, \quad (\text{B35})$$

$$\frac{E_3}{N^2} = \frac{2}{h^2} \sum_{n=0}^{\frac{h-1}{2}} \frac{\tilde{\Gamma} \left[ \frac{2\pi}{h} \left( n + \frac{1}{2} \right) \right]}{\sin^2 \left[ \frac{\pi}{h} \left( n + \frac{1}{2} \right) \right]}. \quad (\text{B36})$$

Let us evaluate the first term in the limit  $h \rightarrow \infty$ ,

$$\begin{aligned} \frac{E_0}{N^2} &= \frac{2\Gamma_0}{h^2} \sum_{n=0}^{\frac{h-1}{2}} \frac{1}{\sin^2 \left[ \frac{\pi}{h} \left( n + \frac{1}{2} \right) \right]} \\ &= \frac{2\Gamma_0}{h^2} \sum_{n=0}^{\frac{h-1}{2}} \sum_{k=-\infty}^{+\infty} \frac{1}{\left[ \frac{\pi}{h} \left( n + \frac{1}{2} \right) - \pi k \right]^2} \\ &\approx \frac{2\Gamma_0}{\pi^2} \sum_{n=0}^{\frac{h-1}{2}} \frac{1}{\left( n + \frac{1}{2} \right)^2} + \frac{4\Gamma_0}{h^2} \sum_{n=0}^{\frac{h-1}{2}} \sum_{k=1}^{\infty} \frac{1}{k^2 \pi^2} + \dots \\ &\approx \Gamma_0 - \frac{\Gamma_0}{h} \left( \frac{4}{\pi^2} - \frac{1}{3} + \dots \right), \end{aligned} \quad (\text{B37})$$

where we have used the result that

$$\begin{aligned} \sum_{n=0}^{\frac{h-1}{2}} \frac{1}{\left( n + \frac{1}{2} \right)^2} &= \frac{\pi^2}{2} - \psi' \left( \frac{h}{2} + 1 \right) \\ &\approx \frac{\pi^2}{2} - \frac{2}{h} + \dots \end{aligned} \quad (\text{B38})$$

The contribution from the second term that arises as a consequence of the nonanalytic contribution to  $\Gamma(\tilde{Q})$  may be evaluated in an analogous fashion:

$$\begin{aligned} \frac{E_1}{N^2} &= -\frac{8\pi^2}{h^3} \sum_{n=0}^{\frac{h-1}{2}} \frac{\left( n + \frac{1}{2} \right)}{\sin^2 \left[ \frac{\pi}{h} \left( n + \frac{1}{2} \right) \right]} \\ &= -\frac{8\pi^2}{h^3} \sum_{n=0}^{\frac{h-1}{2}} \left( n + \frac{1}{2} \right) \sum_{k=-\infty}^{+\infty} \frac{1}{\left[ \frac{\pi}{h} \left( n + \frac{1}{2} \right) - k\pi \right]^2} \\ &\approx -\frac{8}{h} \sum_{n=0}^{\frac{h-1}{2}} \frac{1}{\left( n + \frac{1}{2} \right)} - \frac{16}{h^3} \sum_{n=0}^{\frac{h-1}{2}} \left( n + \frac{1}{2} \right) \sum_{k=1}^{\infty} \frac{1}{k^2} + \dots \\ &\approx -8 \left[ \frac{\ln h}{h} + \frac{1}{h} \left( \gamma + \ln 2 + \frac{\pi^2}{24} \right) + \dots \right], \end{aligned} \quad (\text{B39})$$

where we have used the result that

$$\begin{aligned} \sum_{n=0}^{\frac{h-1}{2}} \frac{1}{\left( n + \frac{1}{2} \right)} &= \gamma + 2 \ln(2) + \psi \left( \frac{h}{2} + 1 \right) \\ &\approx \gamma + 2 \ln(2) + \ln \left( \frac{h}{2} + 1 \right) - \frac{1}{h} + \dots \end{aligned} \quad (\text{B40})$$

The remaining term may be easily evaluated in the limit of large  $h$  by means of the Euler-MacLaurin summation formula

$$\begin{aligned} \frac{E_3}{N^2} &= \frac{2}{h^2} \sum_{n=0}^{\frac{h-1}{2}} \frac{\tilde{\Gamma} \left[ \frac{2\pi}{h} \left( n + \frac{1}{2} \right) \right]}{\sin^2 \left[ \frac{\pi}{h} \left( n + \frac{1}{2} \right) \right]} \\ &\approx \frac{1}{\pi h} \int_0^\pi dK \left[ \frac{\tilde{\Gamma}(K)}{\sin^2(K/2)} \right] \\ &\equiv \frac{C}{h}, \end{aligned} \quad (\text{B42})$$

with

$$C = \frac{1}{\pi} \int_0^\pi dK \left[ \frac{\tilde{\Gamma}(K)}{\sin^2(K/2)} \right]. \quad (\text{B43})$$

Combining the various terms together we obtain

$$\frac{E}{N^2} \approx \Gamma_0 - 8 \left[ \frac{\ln(h)}{h} + \frac{\alpha}{h} \right] + \dots, \quad (\text{B44})$$

where

$$\alpha = \frac{\Gamma_0}{4} \left( \frac{2}{\pi^2} - \frac{1}{6} \right) + \gamma + \ln 2 + \frac{\pi^2}{24} - \frac{C}{4}. \quad (\text{B45})$$

<sup>1</sup>M. B. Taylor and B. L. Gyffory, *J. Phys. Condens. Matter* **5**, 4527 (1993).

<sup>2</sup>A. B. MacIsaac, M.Sc. thesis, Memorial University of Newfoundland, 1992.

<sup>3</sup>J. P. Whitehead, K. De'Bell, and A. B. MacIsaac, in *Quantum Field Theory and Collective Phenomena*, edited by S. De Lillo, F. Khanna, G. Semenoff, and P. Sadano (World Scientific, Singapore, 1993).

<sup>4</sup>T. Garel and S. Doniach, *Phys. Rev. B* **26**, 325 (1982).

<sup>5</sup>Y. Yafet and E. M. Gyorgy, *Phys. Rev. B* **38**, 9145 (1988).

<sup>6</sup>B. Kaplan and G. A. Gehring, *J. Magn. Magn. Mater.* **128**,

111 (1993).

<sup>7</sup>R. Czech and J. Villain, *J. Phys. Condens. Matter* **1**, 619 (1989).

<sup>8</sup>A. B. MacIsaac, J. P. Whitehead, M. C. Robinson, and K. De'Bell, *Physica B* **194-196**, 223 (1994).

<sup>9</sup>A. B. MacIsaac, J. P. Whitehead, K. De'Bell, and K. S. Narayanan, *Phys. Rev. B* **46**, 6387 (1992).

<sup>10</sup>N. M. Fujiki, K. De'Bell, and D. J. W. Geldart, *Phys. Rev. B* **36**, 8512 (1987).

<sup>11</sup>K. De'Bell and J. P. Whitehead, *J. Phys. Condens. Matter* **3**, 2431 (1991).

- <sup>12</sup>S. V. Maleev, Zh. Eksp. Teor. Fiz. **70**, 2374 (1976) [Sov. Phys. JETP **43**, 1240 (1976)].
- <sup>13</sup>N. C. Bartelt, T. L. Einstein, and L. D. Roelofs, Phys. Rev. B **35**, 1776 (1987).
- <sup>14</sup>J. P. Whitehead and K. De'Bell, J. Phys. Condens. Matter **6**, L731 (1994).
- <sup>15</sup>G. A. Gehring and M. Keskin, J. Phys. Condens. Matter **5**, L581 (1993).
- <sup>16</sup>A. Kashuba and V. L. Pokrovsky, Phys. Rev. Lett. **70**, 3155 (1993).